

## **4 Towards Exploring the Proteomic Profile of Rat-1 Fibroblasts on Artificial Extracellular Matrix Proteins**

#### 4.1 Abstract

A first assessment of a biomaterial's biological performance most commonly involves the examination of macroscopic cellular behaviors such as spreading, adhesion, or migration *in vitro*. In this study, we have begun to expand this characterization of cellular response to include an investigation of the alterations in gene transcription and protein expression that occur during cell-biomaterial interaction. Rat-1 fibroblasts were deposited on biomaterials consisting of either adsorbed artificial extracellular matrix (aECM) proteins or fibronectin and allowed to spread for 2 hr. Cellular response was then analyzed in the following three ways: (1) by morphological analysis, through the measurement of cell spread area; (2) by transcriptomic analysis, through evaluation of gene expression levels using microarray technology; and (3) by proteomic analysis, through the utilization of the technique, BONCAT (bio-orthogonal noncanonical amino acid tagging), to detect newly synthesized proteins. Fibronectin and aECM proteins containing the biologically active RGD cell-binding domain were shown to promote cell spreading, and preliminary results indicate that cells deposited on fibronectin showed expression of genes and proteins associated with focal adhesion formation and cytoskeletal organization. Conversely, materials composed of aECM protein harboring a biologically inactive RDG domain did not promote cell spreading, and upregulation of mRNA transcripts encoding for factors involved in apoptosis and proteolysis were detected.

## 4.2 Introduction

New generations of synthetic biomaterials are required to be highly instructive and architecturally complex, interacting with cells and tissues through both chemical and mechanical cues to promote behaviors that aid healing and regeneration [1, 2]. However, despite the vast number of sophisticated biomaterials constructed in the last several years, characterization of cell-biomaterial interaction has remained largely superficial, evaluating phenotypic responses such as the extent of adhesion or migration [3, 4]. Although these measurements provide valuable information regarding cell behavior on materials, a cell interacting with a biomaterial has been shown to exhibit changes in its transcriptomic and proteomic profile [4-7]. Therefore, a more complete description of cell-biomaterial interaction must incorporate both macroscopic and molecular analyses.

Several studies have begun to investigate cell-biomaterial interactions at the molecular level by analyzing changes in intracellular processes such as gene transcription and protein expression. Klapperich and Bertozzi compared the gene expression profile of human fibroblasts (HF) deposited on tissue culture polystyrene to that of HF deposited on three-dimensional collagen-glycosaminoglycan meshes (CGM) and found that over 1000 genes were differentially expressed [7]. HF grown in CGM demonstrated upregulated transcripts for pro-angiogenic factors, chemokines/cytokines, adhesion molecules, and extracellular matrix remodeling genes. As indicated by the authors, upregulation of transcripts related to hypoxia and angiogenesis indicates that careful attention must be given to the pore size of designed materials in order to maintain physiological oxygen levels for cells. Xu and coworkers detected differential expression in 21 proteins when osteoblasts were deposited on bioceramic materials composed of hydroxyapatite (HA)

and hydroxyapatite reinforced with carbon nanotubes (HA-CNT) [6]. Interestingly, even though they noted distinct cellular morphologies of spread cells on HA compared to HA-CNT, they detected similar trends in the ratios of expressed proteins related to cell adhesion (with the exception of vimentin) when compared to a control surface of polystyrene.

Many groups have used both transcriptomic and proteomic techniques to investigate how the surface chemistry of polymeric materials induces an inflammatory response, which ultimately dictates the biocompatibility of implanted materials [8, 9]. These reports have demonstrated notable variability in the production of chemokines, cytokines, and matrix proteins produced by macrophages in response to different polymeric materials. The degree of macrophage activation in response to materials was also found to vary when cells were co-cultured with an increasing density of lymphocytes, indicating that there exists a complex interaction between macrophages and lymphocytes at the biomaterial interface that may need to be addressed in order to improve a material's suitability for clinical use [9]. In another approach, proteomic techniques have been employed to investigate the composition of adsorbed serum proteins on titanium, a metal commonly utilized to generate devices for hip and knee replacements [10, 11].

To foster the development of biomaterials that elicit desired cellular responses, an extensive study of cell-biomaterial interactions must be performed both at the macroscopic and the molecular level. Phenotypic measurements such as the extent of cell spreading and adhesion provide the first indication of a material's biological performance, and combined with further studies evaluating changes in gene and protein

expression, enable a global analysis of cellular response to biomaterials to be attained. This approach allows phenotypic behaviors to be correlated with the expression of multiple proteins and interrogates the extent to which mRNA transcript levels predict protein translation. Moreover, this approach expands the repertoire of *in vitro* testing methods for evaluating material scaffolds for medical applications, and information from these studies can be applied in the design of future materials.

A combined approach that encompasses phenotypic measurements, mRNA microarray analysis, and proteomics has been initiated in this study to further characterize cellular response to aECM proteins. These previously described proteins contain three repeating monomers that each consists of a cell-binding domain derived from fibronectin adjacent to an elastin-like polypeptide (Figure 4-1) [12]. A negative control protein was generated by swapping the position of one amino acid within the cell-binding domain. A phenylalanine residue included in the elastin backbone allows for the replacement of this residue with the photosensitive noncanonical amino acid, *para*-azidophenylalanine ( $pN_3Phe$ ), when expressed in a bacterial host containing a mutant phenylalanyl-tRNA synthetase with relaxed substrate specificity [12]. Incorporation of  $pN_3Phe$  renders proteins intrinsically photoreactive, enabling the degree of crosslinking within protein films to be adjusted by varying the extent of  $pN_3Phe$  incorporation or altering the irradiation dosage at 365 nm [13]. The ability to independently modulate the biochemical (cell binding domain type and density) and mechanical (extent of crosslinking) properties of these materials offers a novel method in which to explore the effects of multiple factors on cellular response.

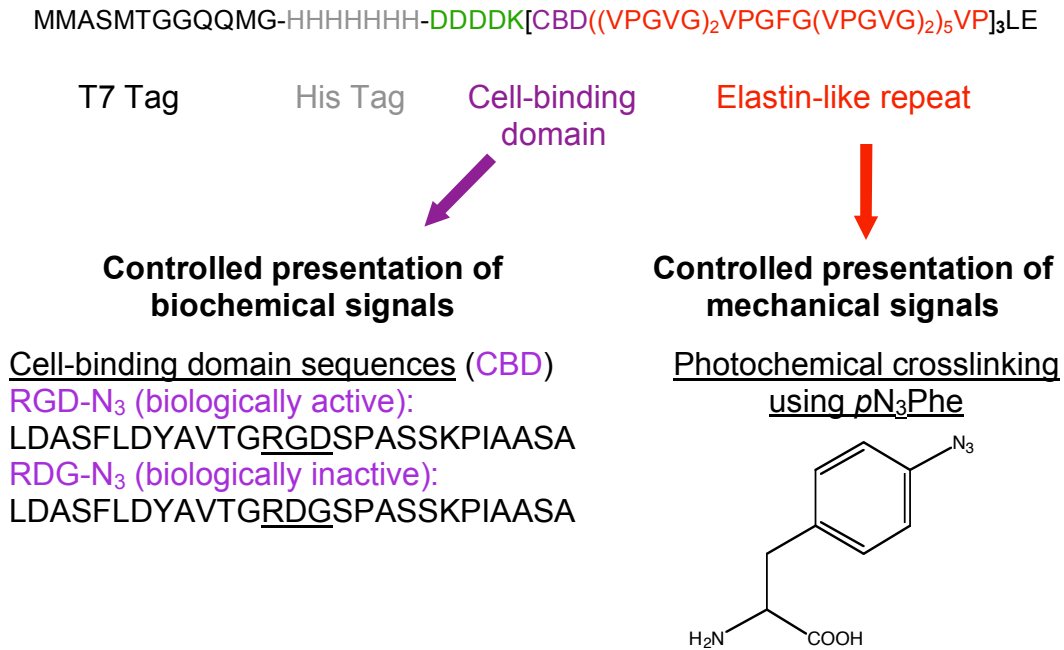


Figure 4-1. aECM protein sequences. Each protein contains a T7 tag, a heptahistidine (His) tag, a cell-binding domain (CBD, purple), and an elastin-like repeat (red). Controlled presentation of biochemical cues can be achieved by mixing the biologically active protein containing the RGD binding domain with the biologically inactive RDG domain. Controlled presentation of mechanical signals is accomplished through the incorporation of *p*N<sub>3</sub>Phe into the elastin subunit, which permits photochemical crosslinking of proteins into films with varying mechanical properties.

In this study, phenotypic measurements were obtained by quantifying cell area after 2 hr of spreading on each artificial protein (RGD-N<sub>3</sub> and RDG-N<sub>3</sub>) as well as surfaces composed of adsorbed fibronectin (FN) and bovine serum albumin (BSA). Affymetrix Genechips were used to examine gene expression from cells deposited on aECM proteins (RGD-N<sub>3</sub>, RDG-N<sub>3</sub>) compared to FN, and the proteomic technique BONCAT was employed to identify newly synthesized proteins produced during spreading on aECM proteins compared to FN (Figure 4-2) [14, 15]. BONCAT permits the enrichment of newly synthesized proteins through the incorporation of a methionine (Met) surrogate, azidohomoalanine (Aha, Figure 4-3), into proteins during a pulse.

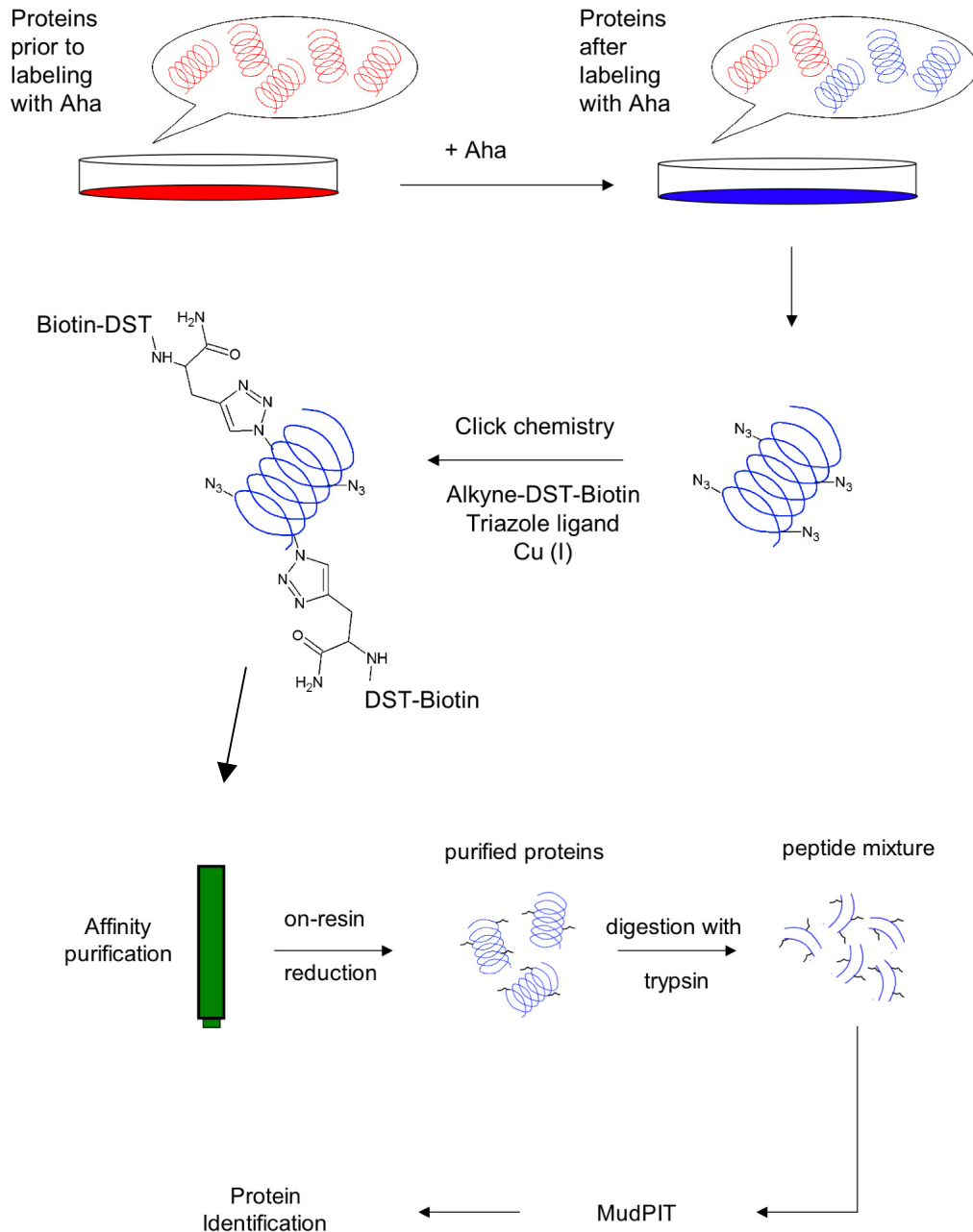


Figure 4-2. Schematic of BONCAT methodology [14]. Prior to labeling with Aha, cells express proteins containing all twenty canonical amino acids (red). After labeling with Aha, all newly synthesized proteins contain Aha (blue), making them distinguishable from preexisting proteins. Cells are lysed and the proteins are coupled to an alkyne disulfide biotin tag (alkyne-DST-Biotin) using click chemistry. Labeled proteins are enriched through affinity chromatography. Proteins are removed from the affinity resin by the addition of  $\beta$ -mercaptoethanol. Reduced proteins are digested with trypsin, and the resulting peptides are analyzed by multi-dimensional protein identification technology (MudPIT) [16]. The observed spectra are then correlated to protein sequences using search engines.

Nascent proteins made during the pulse will contain Aha, making these proteins chemically distinct from preexisting proteins. These proteins are then chemoselectively labeled with an affinity tag using [3+2] copper-catalyzed cycloaddition (“click chemistry”) and resin purified [15]. More specifically, the affinity tag and purification protocol used in this study were recently developed by Jennifer Hodas [19]. Identification of the purified proteins is achieved using multidimensional protein identification technology (MudPIT) and database searching [15, 16]. The combination of these three characterization methods provides a more integrated analysis of cell-aECM protein interaction during early time points of cell spreading.

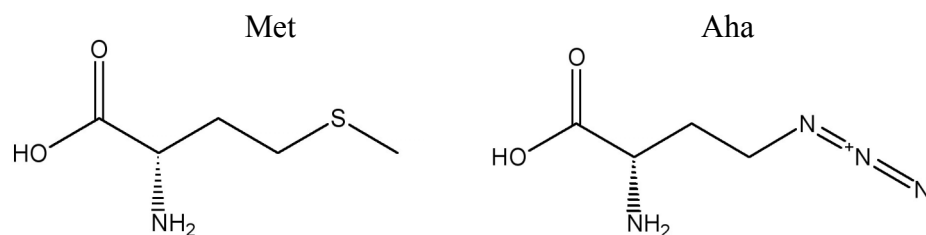


Figure 4-3. Chemical structures of methionine (Met) and azidohomoalanine (Aha).

### 4.3 Materials and Methods

#### 4.3.1 Cell culture

Rat-1 fibroblasts (ATCC, Manassas, VA) were maintained in a 37°C, 5% CO<sub>2</sub> humidified incubator. The cells were grown in Dulbecco’s Modified Eagle Media (DMEM, Invitrogen, Carlsbad, CA) supplemented with 10% fetal bovine serum (Invitrogen) and penicillin/streptomycin (Invitrogen). The media was replaced every 2 d and cells were passaged enzymatically by treatment with 0.05% trypsin with EDTA (Invitrogen).

#### 4.3.2 *Cell synchronization through contact inhibition*

In order to synchronize cells in G0/G1, cells were maintained at confluence for 2 d in DMEM. The extent of cell synchronization, as determined by DNA content, was examined using fluorescence-activated cell sorting (FACS) according to an established protocol [17]. Following incubation at confluence for 2 d, cells were detached using trypsin and transferred to a 15 mL conical tube for centrifugation (1200 rpm, 5 min, 25°C). The supernatant was discarded and 1 mL of chilled 70% ethanol was added dropwise while gently vortexing the cell pellet. Once the cell pellet was fully resuspended, the cell suspension was placed at 4°C for 30 min. The cells were collected by centrifugation (2000 rpm, 5 min, 25°C) and the supernatant was discarded. The cells were resuspended in 1 mL of phosphate buffered saline (PBS) and centrifuged (2000 rpm, 5 min, 25°C). This process was repeated twice. The cells were resuspended in 1 mL of PBS containing 100 µL of 100 µg/mL ribonuclease and left to incubate overnight at room temperature. Following incubation, 400 µL of propidium iodide (50 µg/mL in PBS, Invitrogen) was added to the cell suspension for 15 min. The cell suspension was then passed through a 40 µm filter into a polystyrene round-bottom tube (12 x 75 mm) and analyzed by FACS.

#### 4.3.3 *aECM protein expression and purification*

RGD-N<sub>3</sub> and RDG-N<sub>3</sub> proteins were purified as outlined in Chapter 2.

#### 4.3.4 *Cell spreading experiments*

Cell spreading experiments were performed on adsorbed protein films. Solutions of RGD-N<sub>3</sub> and RDG-N<sub>3</sub> proteins were prepared by dissolving 1 mg of each protein in 1 mL of distilled water. In order to increase protein dissolution, solutions were placed at 4°C overnight. The protein solutions were then sterile filtered (0.2 µm) and transferred to different wells within a 6-well plate and left to adsorb overnight at 4°C. Wells were also prepared containing 1 mL of a 10 µg/mL solution of FN and 1 mL of a 2 mg/mL solution of BSA and incubated overnight at 4°C. Three wells containing each protein solution were prepared per experiment. All wells were rinsed twice with PBS, blocked with 2 mg/mL of BSA for 30 minutes at room temperature, and rinsed three times with PBS. Serum-free DMEM lacking methionine (SFM –Met) was prepared according to a previously described protocol [18] and added to the wells. The medium was then supplemented with either Met or Aha (a gift from Dr. Janek Szychowski) to a final concentration of 2 mM.

Synchronized Rat-1 fibroblasts were incubated for 30 min in SFM –Met to deplete intracellular methionine stores. Following detachment with trypsin, cells were treated with 1 mL of SFM –Met containing 2.3 mg/mL soybean trypsin inhibitor (Sigma, St. Louis, MO). The cells were pelleted via centrifugation and resuspended in 3 mL of SFM –Met. Cells were added at a density of  $1.6 \times 10^5$  cells/well.

For quantification of spread area, images were obtained 2 hr post-seeding using a Nikon Eclipse TE 300 microscope coupled to a Sony CCD color video camera. Images were captured using MetaMorph® imaging software (Molecular Devices, Sunnyvale, CA), and cell areas were manually traced using ImageJ version 1.37v (National Institutes

of Health, Bethesda, MD). For each substrate, at least 200 cells were examined in 3 independent experiments.

#### 4.3.5 *Microarray analysis*

For mRNA microarray analysis, cell spreading was performed using 100 mm diameter Petri dishes coated using identical protein concentrations and blocking procedures as described above. In order to compensate for the increased surface area of the dish, 5 mL of each protein solution was used and the cell density was increased to  $\sim 1.2 \times 10^6$  cells/plate. Synchronized cells were passaged as described above, and cell spreading was conducted in the presence of 2 mM Aha in SFM –Met. Following cell spreading experiments, each plate was rinsed twice with PBS. Isolation of mRNA was performed using the RNeasy Mini kit from Qiagen (Valencia, CA). The protocol outlined in the provided manual for the purification of RNA from animal cells using spin technology was applied. mRNA concentration was determined by measuring the absorbance at 260 nm ( $A_{260}$ ) in a spectrophotometer. An absorbance measurement was also obtained at 280 nm ( $A_{280}$ ) to assess sample purity, as the ratio of the reading at 260 nm and 280 nm provides an estimate of the purity of mRNA with respect to other contaminants (e.g., proteins) that absorb in the UV spectrum. Samples with an  $A_{260}/A_{280}$  ratio between 1.8–2.1 were considered “clean” [7]. Only purified samples with an  $A_{260}/A_{280}$  ratio  $\geq 2$  were submitted for microarray analysis to the Millard and Muriel Jacobs Genetics and Genomics Laboratory at Caltech. Affymetrix GeneChip Rat Genome 230 2.0 arrays (Rat230\_2, Affymetrix, Inc., Santa Clara, CA) were used in all experiments. Each GeneChip Rat Genome 230 2.0 array contains 31,042 probe sets, and

each probe set contains eleven pairs of oligonucleotide probes to measure the transcription level of each sequence presented on the array. The data (rat genes and expressed sequence tags) was analyzed using the Rat Genome Database (RGD, <http://rgd.mcw.edu/>), Rosetta Resolver® version 7.2 (Rosetta Inpharmatics, Inc., Seattle, WA), and Microsoft Excel. The ratio-builder function in Resolver® was used to perform ratio experiments, and transcripts with intensity ratios (either  $\text{intensity}^{\text{RGD/RDG}}/\text{intensity}^{\text{FN}}$  or  $\text{intensity}^{\text{RGD}}/\text{intensity}^{\text{RDG}}$ ) having a  $P$  value  $\leq 0.01$  with a  $\geq 2.0$ -fold change were considered differentially expressed.

#### 4.3.6 *Cell lysis and protein extraction for proteomic analysis*

Preliminary proteomic analysis was performed using FN-coated plates only. Cell spreading was performed using 100 mm diameter Petri dishes coated with FN and blocked with BSA as described above. SFM –Met was added to the plates and supplemented with either 2 mM Met or Aha. Synchronized cells were passaged as described above and deposited at a density of  $\sim 1.2 \times 10^6$  cells/plate. Following cell spreading experiments, each plate was rinsed twice with PBS. The cells were lysed directly on the plate according to a communicated protocol [19] by the addition of 250  $\mu\text{L}$  of 1% (w/v) SDS in PBS-PI (PBS, pH = 7.6, supplemented with EDTA-free complete protease inhibitor cocktail (PI), Roche Applied Science, Indianapolis, IN). The cell lysates were treated with 1  $\mu\text{L}$  of benzonase ( $> 500$  U, Sigma), transferred to a microcentrifuge tube, and vortexed for 30–60 seconds. In order to achieve complete cell lysis and protein denaturation, the samples were sonicated in a bath sonicator for 10 min and boiled at 96–100°C for 10 min. The samples were cooled to room temperature and

adjusted to 0.1% SDS by the addition of 2.25 mL of PBS-PI. Moreover, 20  $\mu$ L of 20% Triton X-100 was added to each sample. The samples were then centrifuged (2000g, 5 min, 4°C) and the supernatants were transferred to new tubes.

Cell lysates were labeled with an alkyne-disulfide-biotin tag (DST) using click chemistry [19]. Following a protocol described by Jennifer Hodas [19], each sample (5 mL) was incubated with the following reagents at 4°C overnight with constant agitation: 5  $\mu$ L of 200 mM triazole ligand in dimethyl sulfoxide, 2.5  $\mu$ L of 50 mM DST, and 50  $\mu$ L of 10 mg/mL CuBr. The reacted lysates were centrifuged (2000g, 5 min, 4°C) and the supernatants were transferred to new tubes. Excess unreacted DST was removed by subjecting the samples to gel filtration using PD-10 columns (GE Healthcare, Waukesha, WI). Each column was equilibrated with 25 mL of 0.05% SDS in PBS (pH = 7.6), and the protein fractions were eluted in 3.5 mL of 0.05% SDS in PBS (pH = 7.6). The desalted samples were boiled at 96–100°C for 10 min and cooled to room temperature before performing the affinity purification procedure.

#### 4.3.7 *Affinity purification*

NeutrAvidin resin (Pierce, Rockford, IL) was used to separate DST-labeled proteins from unlabeled proteins following desalting [19]. The resin was first washed with PBS (pH = 7.6) at room temperature with constant agitation for 5 min. The resin was then collected by centrifugation (2000g, 5 min, 4°C) and the supernatant was removed. This washing procedure was repeated twice. Before adding the desalted samples to the washed resin, the samples were adjusted to 1% (v/v) NP-40 (Nonidet P40, Roche) and 0.05% SDS in PBS-PI. The samples were incubated with resin for 24 hours at

room temperature with constant agitation. The resin was collected by centrifugation (2000g, 5 min, 4°C) and the supernatants were removed. The resin was washed twice for 5 minutes at room temperature with 1% NP-40, then washed twice with PBS (pH = 7.6), and finally washed with freshly made 50 mM ammonium bicarbonate. Between each washing step the samples were centrifuged (2000g, 5 min, 4°C) and the supernatants were discarded. The resin was transferred to a microcentrifuge tube using 1 mL of 50 mM ammonium bicarbonate and centrifuged (2000g, 5 min, 4°C). The supernatants were discarded and the resin was treated with 500 µL of 2% β-mercaptoethanol in 50 mM ammonium bicarbonate for 1 hour at room temperature with constant agitation. The samples were centrifuged (2000g, 5 min, 4°C) and the supernatants containing the reduced proteins were saved. A second reduction step was performed for 30 min under identical conditions and the reduced eluates were combined. This combined sample was transferred to an empty chromatography spin-column (Bio-Rad Laboratories, Hercules, CA) and centrifuged (4000g, 2 min, 4°C) to remove any remaining resin from the solution.

#### *4.3.8 Sample preparation for tandem mass spectrometry analysis*

The eluate volume was reduced to ~ 100–200 µL by vacuum centrifugation. The samples were further concentrated via acetone precipitation. Proteins were precipitated by the addition of chilled acetone and the samples stored at -20°C overnight before centrifugation (14000g, 10 min, 4°C). The supernatants were discarded and the pellets were dried at room temperature for 1 hr. The pellets were resuspended in 40 µL of 8 M urea in 100 mM Tris-HCl (pH = 8.5). Each sample was further reduced by incubation

with 0.5  $\mu\text{L}$  of 500 mM tris(2-carboxyethyl)phosphine (TCEP) for 20 min at room temperature with constant agitation. Cysteine residues were alkylated by the addition of 0.9  $\mu\text{L}$  of 500 mM iodoacetamide. Proteolysis was initiated by incubating the samples with Endoproteinase Lys-C (1  $\mu\text{L}$  of 0.1  $\mu\text{g}/\mu\text{L}$ , Roche) for 4 hours at 37°C with constant agitation. Following digestion, the samples were diluted to 2 M urea by adding 120  $\mu\text{L}$  of 100 mM Tris-HCl (pH = 8.5). The samples were treated with 1.6  $\mu\text{L}$  of 100 mM  $\text{CaCl}_2$  and further digested with 1.5  $\mu\text{L}$  of 0.5  $\mu\text{g}/\mu\text{L}$  trypsin (Promega, Madison, WI) at 37°C for 16 hr with constant agitation. The digestion was quenched by the addition of 10  $\mu\text{L}$  of 90% (v/v) formic acid.

Salts and detergents were removed by subjecting the samples to high performance liquid chromatography (HPLC). More specifically, peptides were desalted using the Alliance-HT HPLC (Waters Corporation, Milford, MA) equipped with a C8 peptide MacroTrap column (Microm Bioresources, Auburn, USA; 3 $\times$ 8 mm; 200 mg capacity). A 40-min desalting step was performed for each sample. The desalting step was initiated with a 10-min wash step with 0.2% formic acid in water (Buffer A). A gradient was then started with Buffer A and gradually increased to achieve 90% of Buffer B (Buffer B = 0.2% formic acid in acetonitrile) within 23 min at a flow rate 250  $\mu\text{L}/\text{min}$ . The gradient was stopped and the column was flushed with 100% of Buffer A for 7 min. A blank (water) run was performed between each sample. Fractions containing the eluted peptides were analyzed by MudPIT [16] at the Proteomic Exploration Laboratory at Caltech.

#### 4.3.9 *Analysis of tandem mass spectrometry data*

The obtained tandem mass spectra were searched against the International Protein Index (IPI: Rat database version 3.47) using search engines Sorcerer (SageN Research Products, San Jose, CA) and MASCOT (Matrix Science, homepage: <http://www.matrixscience.com>) with a parent ion tolerance of 20 ppm. Alkylation of cysteine residues with iodoacetamide was specified as a fixed modification, while oxidation of methionine and acetylation of lysine and the N-terminus were specified as variable modifications. Variable methionine modifications related to the incorporation of Aha (loss of 4.986324 amu compared to Met) and DST labeling (+195.075623 amu) were also included. Protein identifications were viewed using Scaffold (version 01\_07\_00, Proteome Software, Inc., Portland, OR), and identifications were accepted if established with greater than 80% probability for peptides and greater than 99% probability for proteins (containing a minimum of 2 uniquely identified peptides). Probabilities were assigned using Peptide and Protein Prophet algorithms [20].

Gene-annotation enrichment analysis and pathway analysis were performed by importing the list of identified proteins in the form of a rat gene ID list into DAVID (Database for Annotation, Visualization, and Integrated Discovery, National Institute of Allergy and Infectious Disease, <http://david.abcc.ncifcrf.gov/home.jsp>). A modified Fisher exact *P* value of 0.05 was used in all tests.

## 4.4 Results and Discussion

### 4.4.1 *Cell synchronization through contact inhibition*

Synchronizing cells using contact inhibition relies on the natural cessation of cell division and migration as a result of physical contact with other cells or colonies [21]. This method of synchronization has been widely studied and shown to synchronize several types of fibroblasts [22, 23]. In this study, cell cycle synchronization in the G0/G1 stage was achieved by maintaining Rat-1 cells at confluence for 2 d in 100 mm diameter Petri dishes. The efficiency of synchronization in G0/G1 was evaluated by propidium iodide staining of cellular DNA and FACS analysis. Figure 4-4 shows FACS data obtained from examination of the DNA content of both unsynchronized (70% confluent) and synchronized (2 d at confluence) cultures. Unsynchronized cells (Figure 4-4 (A)) show three distinct cell populations (M1, M2, M3) that correspond to different stages of the cell cycle (G0/G1, S, G2/M). Maintaining cells at confluence for 2 d results in an increase in the percentage of cells in G0/G1, from 54% to 86%, and a corresponding decrease in the percentage of cells in S and G2/M (Figure 4-4 (B)). Allowing cells to remain at confluence for a third day only increased synchronization in G0/G1 by 1% (data not shown); however, this increase was accompanied by an increase in the number of apoptotic cells observed by FACS. Thus, prior to experiments, cells were kept at confluence for 2 d to achieve sufficient synchronization without inducing undesired apoptosis. Performing subsequent analyses on synchronized cells ensures that transcriptional and proteomic changes reflect differences in cell-material interactions and not changes in the cell cycle.

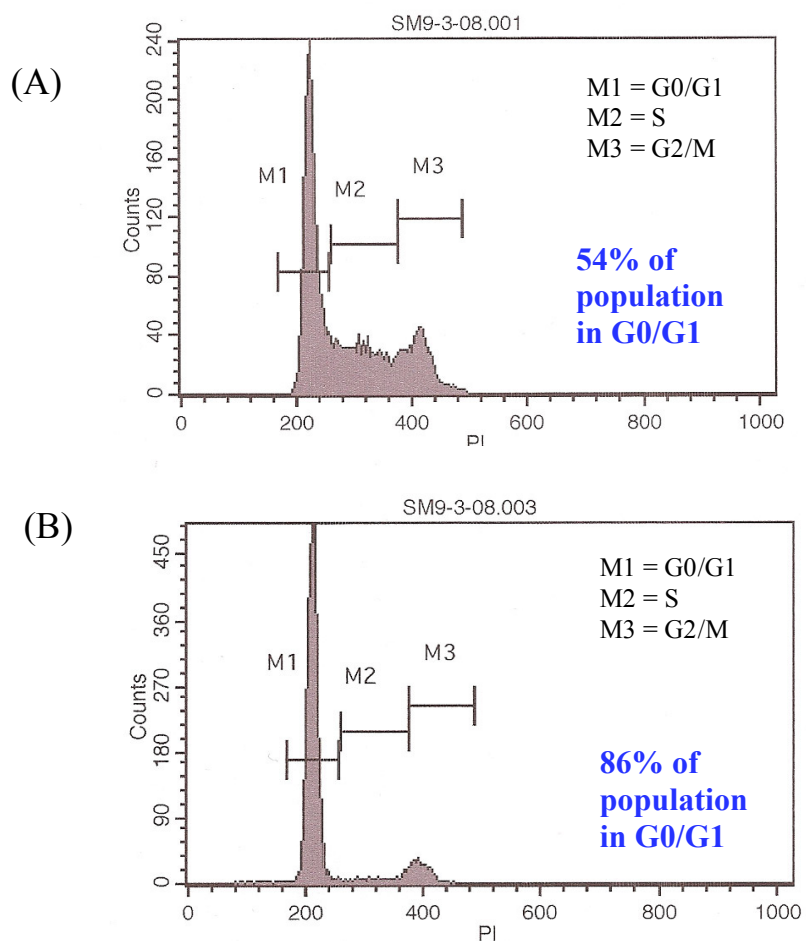


Figure 4-4. FACS analysis of Rat-1 fibroblasts before (A) and after (B) cell synchronization by contact inhibition. The cell population in (A) was  $\sim 70\%$  confluent before FACS analysis, and the cell population in (B) was maintained at confluence for 2 d before FACS analysis. An increase in the percentage of cells in G0/G1 (54% to 86%) was observed as result of maintaining cells at confluence for 2 d.

#### 4.4.2 Cell spreading results

To examine the sequence-specific nature of Rat-1 fibroblast spreading on aECM proteins in the presence of 2 mM Aha, a series of cell spreading experiments was performed on adsorbed protein films. Rat-1 cells attained a greater average spread area and exhibited well-spread morphologies on RGD- $N_3$  films after 2 hr of spreading compared to the RDG- $N_3$  films (Figures 4-5 and 4-6). Cell areas achieved on the RGD-

$N_3$  samples resemble those results obtained for FN, whereas the cell areas measured on the RDG- $N_3$  samples matched areas measured on the negative control of BSA (Figure 4-6). The observation that Rat-1 cells spread on RGD- $N_3$  films and not on RDG- $N_3$  films indicates that cells recognize the RGD cell-binding domain specifically. These results are in accordance with previous experiments performed in the presence of Met at longer time points ( $t = 4$  hr) [12], demonstrating that Aha does not affect cell spreading.

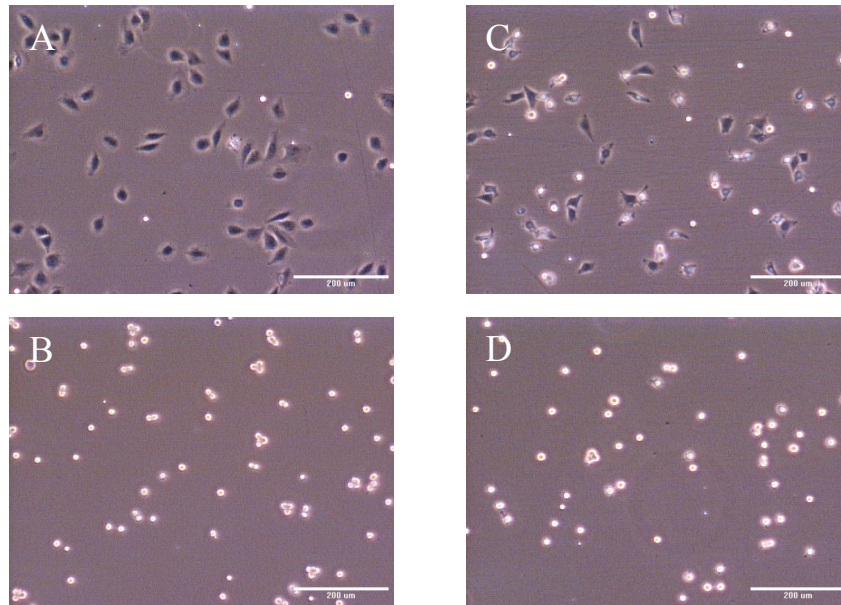


Figure 4-5. Images of cells captured after 2 hours of spreading. (A) FN, (B) BSA, (C) RGD- $N_3$ , and (D) RDG- $N_3$ . Scale bars represent 200  $\mu\text{m}$ .

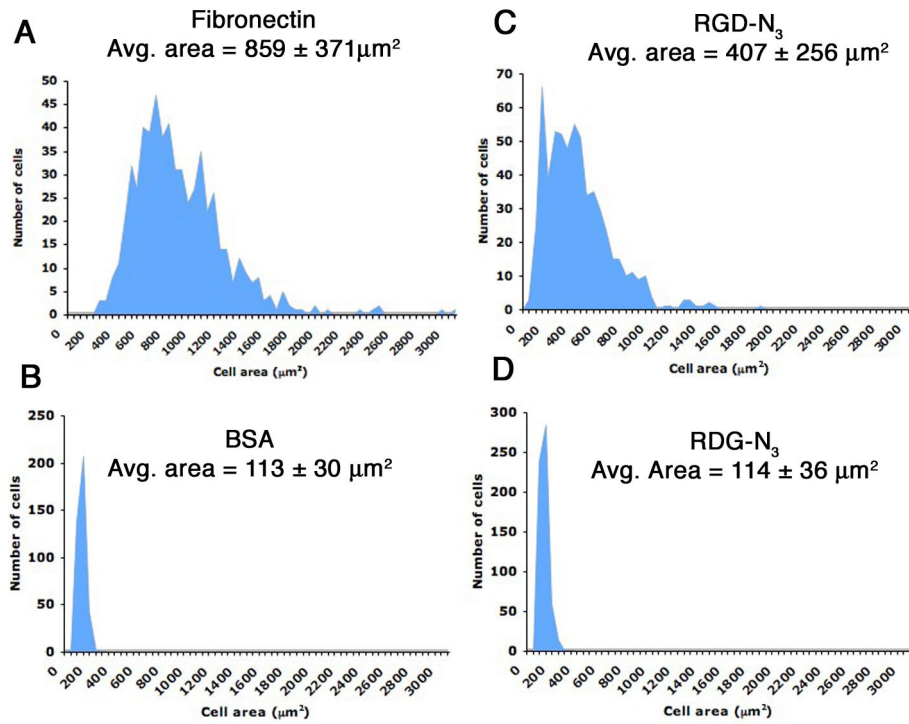


Figure 4-6. Rat-1 cell spread areas on (A) FN, (B) BSA, (C) RGD- $\text{N}_3$ , and (D) RDG- $\text{N}_3$ . The observation that Rat-1 cells spread well on RGD- $\text{N}_3$  films and not on RDG- $\text{N}_3$  films indicates that cells recognize the RGD cell-binding domain specifically in the presence of Aha.

#### 4.4.3 mRNA microarray results

We have begun to compare the global transcriptional profile of Rat-1 fibroblast cells deposited on RGD- $\text{N}_3$  and RDG- $\text{N}_3$  proteins compared to FN using mRNA microarrays. Following cell spreading, mRNA was successfully extracted from cells and  $\geq 2 \mu\text{g}$  of purified mRNA was obtained for each material investigated. All mRNA samples were processed and hybridized to Affymetrix GeneChips at the Muriel and Milliard Jacobs Center for Genes and Genomic Research at Caltech. One microarray chip per protein type was analyzed. The data collected from the microarray experiments was uploaded to the Resolver server at Caltech and analyzed. All data analysis was performed

utilizing built-in features of the Rosetta Resolver® Gene Expression Data Analysis System.

Ratio experiments were conducted using the Rosetta Resolver® Ratio Builder function to compare the expression levels of mRNA transcripts from cells deposited on different proteins. Two ratio experiments were performing using FN as a baseline with RGD-N<sub>3</sub> and RDG-N<sub>3</sub> as experimental samples (FN versus RGD, and FN versus RDG), and one ratio experiment was conducted with RDG-N<sub>3</sub> set as the baseline and RGD-N<sub>3</sub> as the experimental sample (RDG versus RGD). The data sets were then sorted using Excel to identify differentially expressed transcripts with  $\geq 2.0$ -fold change and a calculated *P* value  $\leq 0.01$ .

The extent to which aECM proteins elicit biological responses similar to that of the natural protein FN during early time points of cell spreading was examined by comparing the expression level of mRNA transcripts related to the process of cell-matrix adhesion. Table 4-1 shows a comparison of the fold changes between different genes for a selected number of differentially expressed transcripts and for other transcripts known to mediate cell spreading and focal adhesion formation [24]. These preliminary results show that many of the transcripts that encode for proteins involved in focal adhesion formation were not differentially expressed under these conditions.

Adhesion-related transcripts that were found to be differentially expressed on both RGD-N<sub>3</sub> and RDG-N<sub>3</sub> compared to FN include myosin regulatory light chain,  $\alpha$ -actinin, and tropomyosin. A possible explanation for the observed downregulation in these transcripts detected on the RGD-N<sub>3</sub> surface compared to FN could involve the kinetics of the cellular spreading on RGD-N<sub>3</sub> proteins. Previous experiments using RGD-N<sub>3</sub> proteins

demonstrate that cells achieve a higher average spread area at longer time points (516  $\mu\text{m}^2$  versus 407  $\mu\text{m}^2$ ) [12], suggesting that cells on RGD- $\text{N}_3$  in this experiment may exist in an early phase of spreading compared to FN samples. This early phase of spreading may only induce the production of a smaller number of transcripts that are needed to manufacture intracellular proteins to facilitate spreading, which correlates with the observation that cells attain a lower average spread area compared to FN at this time point. Moreover, it is important to note that cell areas were acquired following 2 hr of spreading while mRNA was extracted from cells after only 1 hr of spreading. The difference in cell spread areas between these surfaces at an earlier time point are likely to be greater than reported at 2 hr, which may also explain the differential expression of these genes. The downregulation of these transcripts on the RDG- $\text{N}_3$  surface compared to FN is expected, as the biologically inactive RDG domain does not promote spreading at any time point [12].

Ubiquitin D, a protein involved in mediating proteolysis, was found to be upregulated on both RGD- $\text{N}_3$  and RDG- $\text{N}_3$  samples compared to FN, suggesting that cells deposited on aECM proteins may be undergoing a higher level of protein degradation than cells deposited on FN [25]. Moreover, a downregulation in the transcription of the anti-apoptotic factor Bcl2-like 2 on RDG- $\text{N}_3$  samples implies that seeding cells on this surface may result in increased cell death [26]. Since anchorage-dependent cells like fibroblasts require contact with an underlying substrate for survival [27], the inability of cells to spread on RDG- $\text{N}_3$  samples complements the suppression of anti-apoptotic signals detected by microarray analysis. Both technical and biological replicates of these experiments are needed to validate the identification of differentially

expressed genes and to further investigate the role of other differentially expressed transcripts in cell-biomaterial interactions.

Table 4-1. Selected list of differentially expressed mRNA transcripts from ratio experiments with FN, RGD-N<sub>3</sub>, and RDG-N<sub>3</sub> samples. All upregulated transcripts are shown in red, all downregulated transcripts are shown in blue, and dashed lines show transcripts that were not differentially expressed.

Protein product of mRNA transcript	FN vs. RGD	FN vs. RDG	RDG vs. RGD
actin	---	---	---
$\alpha$ -actinin	↓ 3 fold	↓ 3.9 fold	---
Bcl2-like 2	---	↓ 4.7 fold	---
collagen	---	---	---
fibroblast growth factor receptor 2	---	---	↑ 7.9 fold
fibronectin	---	---	---
filamin	---	---	---
focal adhesion kinase	---	---	---
heparin-binding EGF-like growth factor	↓ 2.7 fold	↓ 4.2 fold	---
lamin	---	---	---
laminin	---	---	---
myosin	---	---	---
myosin regulatory light chain	↓ 2.4 fold	↓ 4.1 fold	---
paxillin	---	---	---
profilin	---	---	---
Rho family GTPase 3	---	↓ 2.2 fold	---
Rho guanine nucleotide exchange factor	---	---	↑ 3.4 fold
talin	---	---	---
tropomyosin	↓ 3.3 fold	↓ 5.5 fold	---
ubiquitin D	↑ 3.3 fold	↑ 3.8 fold	---
vinculin	---	---	---

#### 4.4.4 BONCAT results

Preliminary experiments investigating the proteomic profile of spreading Rat-1 fibroblasts on FN-coated surfaces have been performed. Rat-1 fibroblasts were deposited on adsorbed FN films and allowed to spread for 2 hr in the presence of 2 mM Aha or 2 mM Met. Cells were lysed in order to collect cellular proteins, and the extracted proteins were labeled with an affinity tag using click chemistry. Labeled proteins were affinity purified using NeutrAvidin resin and recollected for identification by performing an on-

resin reduction with  $\beta$ -mercaptoethanol. Purified proteins obtained from the reduction step were analyzed by MudPIT [16].

Both MASCOT and Sorcerer search engines were used to identify proteins from obtained mass spectra. In order to be classified as newly synthesized using the incubation step with Aha, proteins were identified by a minimum of 2 unique peptides and had a greater than 99% protein identification probability. Although previous reports have required that peptides contain an Aha-derived modification to be considered newly translated, we have not included this restraint in our study as the only proteins identified in the Met sample, with the exception of a single ribosomal protein (ribosomal protein S27a), were derived from contaminants (e.g. trypsin, human keratins, and BSA). Therefore, all proteins identified in the Aha sample were considered newly synthesized during cell spreading experiments.

In the 2-hr interval of cell spreading examined, a total of 88 unique proteins were identified in the Aha sample. In particular, proteins shown to be important in mediating adhesion between cells and the extracellular matrix, such as vinculin, talin, filamin, vimentin, and  $\alpha$ -actinin, were identified (Table 4-2) [24]. Examples of other proteins identified include actin,  $\beta$ -tubulin, and isoforms of myosin light and heavy chains. Proteins involved in translation and cell proliferation were also identified, such as ribosomal proteins (40S ribosomal proteins S6 and S8, and 60S ribosomal protein L7a) and isomerases (protein disulfide-isomerase A3 and peptidyl-prolyl cis-trans isomerase A), respectively [6]. In accordance with preliminary microarray results,  $\alpha$ -actinin, myosin regulatory light chain 2, and tropomyosin were detected as proteins synthesized during the Aha pulse.

Table 4-2. List of identified newly synthesized proteins shown to play a role in cell-ECM interactions, focal adhesion formation, and cytoskeletal reorganization [24].

Identified newly synthesized proteins important in cell-ECM interactions and cytoskeletal reorganization	
	actin, cytoplasmic 2 $\alpha$ -actinin-1 collagen, type 1, $\alpha$ 1 collagen, $\alpha$ -2(I) chain cofilin-1 filamin-A isoform I of fibronectin laminin $\beta$ -1 myosin-9 myosin-10 myosin regulatory light chain 2-B profilin-1 talin tropomyosin $\alpha$ -4 chain isoform of tubulin $\beta$ -3 chain isoform of tubulin $\beta$ -5 chain vimentin vinculin

Gene ontology analysis of identified proteins in the Aha sample was performed using DAVID. The gene IDs for the identified proteins were determined using the RGD and imported as a gene list. The DAVID program sorted the list into bins according to Panther annotation terms [28]. Figure 4-7 shows an example of an analysis conducted using the identified proteins and sorted with Panther annotation terms restricted to “molecular function”. The analysis from DAVID showed that a significant number of identified proteins are involved in the regulation of the actin cytoskeleton. This result correlates with phenotypic observations demonstrating that cells are well spread on FN, as spreading and extension of the cell membrane involves the reorganization of the actin cytoskeleton and the formation of new sites of actin polymerization [29]. A majority of identified proteins were binned into the category of nucleic acid binding, a result that corresponds to observations made from previous dye-labeling experiments illustrating

that newly synthesized proteins are highly concentrated near the nucleus and in the nucleoli [18]. Overall, these preliminary results also highlight the diversity in molecular function of proteins identified using BONCAT that provide a more integrated characterization of cell-biomaterial interactions.

Term	RT	Genes	Count	%	P-Value
MF00261:Actin binding cytoskeletal protein	<a href="#">RT</a>		18	21.4	1.5E-9
MF00091:Cytoskeletal protein	<a href="#">RT</a>		15	17.9	7.5E-7
MF00077:Chaperone	<a href="#">RT</a>		8	9.5	3.5E-6
MF00262:Non-motor actin binding protein	<a href="#">RT</a>		15	17.9	1.5E-3
MF00250:Serine protease inhibitor	<a href="#">RT</a>		11	13.1	2.7E-3
MF00236:Exoribonuclease	<a href="#">RT</a>		5	6.0	3.0E-3
MF00230:Actin binding motor protein	<a href="#">RT</a>		8	9.5	3.2E-3
MF00210:Hsp 90 family chaperone	<a href="#">RT</a>		3	3.6	5.2E-3
MF00219:Annexin	<a href="#">RT</a>		4	4.8	7.2E-3
MF00209:Hsp 70 family chaperone	<a href="#">RT</a>		3	3.6	1.0E-2
MF00087:Transfer/carrier protein	<a href="#">RT</a>		6	7.1	1.5E-2
MF00169:Other isomerase	<a href="#">RT</a>		4	4.8	1.6E-2
MF00254:Actin and actin related protein	<a href="#">RT</a>		6	7.1	1.7E-2
MF00188>Select calcium binding protein	<a href="#">RT</a>		5	6.0	2.0E-2
MF00166:Isomerase	<a href="#">RT</a>		4	4.8	2.2E-2
MF00075:Ribosomal protein	<a href="#">RT</a>		9	10.7	2.6E-2
MF00042:Nucleic acid binding	<a href="#">RT</a>		28	33.3	2.9E-2
MF00099:Small GTPase	<a href="#">RT</a>		10	11.9	4.0E-2

Figure 4-7. Gene ontology analysis of newly synthesized proteins in Aha-treated samples using DAVID. Of the 88 candidate proteins submitted, 84 were assigned DAVID IDs, and 69 were included in the chart. Several proteins are listed in multiple bins. Each molecular function (MF) annotation term is listed, followed by a link for related terms (RT). The number and percentage of genes included in the annotation binning is listed along with the calculated *P* value for each term.

Pathway analysis was also performed using DAVID to determine whether certain cellular pathways were considered enriched within the provided gene list as compared to random chance. Figure 4-8 shows the KEGG (Kyoto Encyclopedia for Genes and Genomes, <http://www.genome.jp/kegg/>) pathways that were detected with a modified Fisher exact  $P$  value  $\leq 0.05$ . This analysis further supports the observation that cellular processes including focal adhesion formation, regulation of the actin cytoskeleton, as well as extracellular matrix (ECM)-receptor interactions are likely occurring within the cell during spreading on FN. In addition to processes related to cell-ECM interactions, metabolic processes were also considered enriched including glycolysis/gluconeogenesis, pyruvate metabolism, and carbon fixation.

Category	Term	RT	Genes	Count	%	P-Value
KEGG_PATHWAY	<a href="#">Glycolysis / Gluconeogenesis</a>	RT		6	7.1	1.5E-4
KEGG_PATHWAY	<a href="#">Focal adhesion</a>	RT		9	10.7	8.2E-4
KEGG_PATHWAY	<a href="#">Cell Communication</a>	RT		7	8.3	2.1E-3
KEGG_PATHWAY	<a href="#">Antigen processing and presentation</a>	RT		5	6.0	1.8E-2
KEGG_PATHWAY	<a href="#">Carbon fixation</a>	RT		3	3.6	2.0E-2
KEGG_PATHWAY	<a href="#">Regulation of actin cytoskeleton</a>	RT		7	8.3	2.4E-2
KEGG_PATHWAY	<a href="#">ECM-receptor interaction</a>	RT		4	4.8	4.2E-2
KEGG_PATHWAY	<a href="#">Ribosome</a>	RT		4	4.8	4.5E-2
KEGG_PATHWAY	<a href="#">Pyruvate metabolism</a>	RT		3	3.6	4.5E-2

Figure 4-8. Pathway analysis of the imported list from Aha-treated samples using DAVID. The associated KEGG pathway is listed as a term along with a link for related terms (RT). The number and percentage of genes included in the annotation binning is listed along with the calculated  $P$  value for each pathway. Of the 84 proteins assigned DAVID IDs, 29 were included in the pathway analysis. Several proteins are listed in multiple pathways.

#### 4.5 Conclusions and Future Work

Preliminary experiments have been conducted to correlate the phenotypic behavior of cells deposited on aECM proteins and FN at early time points of cell

spreading with intracellular changes in gene transcription and protein translation. Cell spreading experiments were performed to provide a quantitative assessment of cell morphology on different surfaces, and changes in mRNA transcript levels were analyzed using microarray technology. The identification of newly synthesized proteins produced during cell-biomaterial interaction was accomplished by employing the proteomic technique, BONCAT. These experiments provide valuable information regarding cell-biomaterial interaction that can be used in the design of future aECM proteins.

Cell spreading experiments demonstrated that cells attained different degrees of spreading on aECM proteins and FN. Cells appeared well-spread on FN and attained the highest average spread area on these surfaces. Cells also appeared spread on RGD-N<sub>3</sub>, though they attained a slightly lower average spread area at this time point compared to FN. In contrast, cells did not spread and remained round with a low average spread area on RDG-N<sub>3</sub> samples. These differences in morphological behavior were reflected in the transcription levels of three mRNA transcripts:  $\alpha$ -actinin, myosin regulatory light chain 2, and tropomyosin. Differences in the expression levels of other mRNA transcripts that encode for proteins involved in cell-ECM interactions were not detected at this time point. Future studies with microarrays will use both biological and technical replicates at a time point matching that for the cell spreading and BONCAT experiments to validate these conclusions and to examine the role of other differentially expressed mRNA transcripts in mediating cell spreading on aECM proteins.

BONCAT experiments were initiated using FN samples, and 88 unique proteins were identified as newly synthesized during the Aha pulse. Proteins involved in focal adhesion formation and the regulation of the actin cytoskeletal were found to be newly

synthesized, as were other proteins involved in metabolic processes such as glycolysis and gluconeogenesis. Future BONCAT experiments will compare the proteomic profiles of cells deposited on aECM proteins with varying biological and mechanical properties.

#### 4.6 References

1. Maskarinec, S.A., and D.A. Tirrell, *Protein engineering approaches to biomaterials design*. *Current Opinion in Biotechnology*, 2005. **16**(4): 422-426.
2. Lutolf, M.P., and J.A. Hubbell, *Synthetic biomaterials as instructive extracellular microenvironments for morphogenesis in tissue engineering*. *Nature Biotechnology*, 2005. **23**(1): 47-55.
3. Heilshorn, S.C., J.C. Liu, and D.A. Tirrell, *Cell-binding domain context affects cell behavior on engineered proteins*. *Biomacromolecules*, 2005. **6**(1): 318-323.
4. Allen, L.T., et al., *Interaction of soft condensed materials with living cells: Phenotype/transcriptome correlations for the hydrophobic effect*. *Proceedings of the National Academy of Sciences of the United States of America*, 2003. **100**(11): 6331-6336.
5. Gallagher, W.M., et al., *Molecular basis of cell-biomaterial interaction: Insights gained from transcriptomic and proteomic studies*. *Biomaterials*, 2006. **27**(35): 5871-5882.
6. Xu, J.L., et al., *Comparative proteomics profile of osteoblasts cultured on dissimilar hydroxyapatite biomaterials: An iTRAQ-coupled 2-D LC-MS/MS analysis*. *Proteomics*, 2008. **8**(20): 4249-4258.
7. Klapperich, C.M., and C.R. Bertozzi, *Global gene expression of cells attached to a tissue engineering scaffold*. *Biomaterials*, 2004. **25**(25): 5631-5641.
8. Jones, J.A., et al., *Proteomic analysis and quantification of cytokines and chemokines from biomaterial surface-adherent macrophages and foreign body*

- giant cells*. Journal of Biomedical Materials Research Part A, 2007. **83A**: 585-596.
9. Chang, D.T., et al., *Lymphocyte/macrophage interactions: Biomaterial surface-dependent cytokine, chemokine, and matrix protein production*. Journal of Biomedical Materials Research Part A, 2008. **87A**(3): 676-687.
  10. Derhami, K., et al., *Proteomic analysis of human skin fibroblasts grown on titanium: Novel approach to study molecular biocompatibility*. Journal of Biomedical Materials Research, 2001. **56**(2): 234-244.
  11. Williams, D., *The golden anniversary of titanium biomaterials*. Medical Device Technology, 2001. **12**(7): 8-11.
  12. Carrico, I.S., et al., *Lithographic patterning of photoreactive cell-adhesive proteins*. Journal of the American Chemical Society, 2007. **129**(16): 4874-4875.
  13. Nowatzki, P.J., et al., *Mechanically tunable thin films of photosensitive artificial proteins: Preparation and characterization by nanoindentation*. Macromolecules, 2008. **41**(5): 1839-1845.
  14. Dieterich, D.C., et al., *Selective identification of newly synthesized proteins in mammalian cells using bioorthogonal noncanonical amino acid tagging (BONCAT)*. Proceedings of the National Academy of Sciences of the United States of America, 2006. **103**(25): 9482-9487.
  15. Dieterich, D.C., et al., *Labeling, detection and identification of newly synthesized proteomes with bioorthogonal non-canonical amino-acid tagging*. Nature Protocols, 2007. **2**: 532-540.

16. Delahunty, C.M. and J.R. Yates, *MudPIT: multidimensional protein identification technology*. Biotechniques, 2007. **43**: 563-569.
17. Diamond, R., and S. DeMaggio, eds., *In Living Color*. Protocols in Flow Cytometry and Cell Sorting, 2000, New York: Springer Lab Manuals.
18. Beatty, K.E., et al., *Fluorescence visualization of newly synthesized proteins in mammalian cells*. Angewandte Chemie-International Edition, 2006. **45**(44): 7364-7367.
19. Hodas, J.L., *Personal communication*, 2009.
20. Nesvizhskii, A.I., et al., *A statistical model for identifying proteins by tandem mass spectrometry*. Analytical Chemistry, 2003. **75**(17): 4646-4658.
21. Jackman, J., and P.M. O'Connor, *Methods for synchronizing cells at specific stages of the cell cycle*. Current Protocols in Cell Biology, 2001. 8.3.
22. Holley, R.W., and J.A. Kiernan, *Contact Inhibition of Cell Division in 3T3 Cells*. Proceedings of the National Academy of Sciences of the United States of America, 1968. **60**(1): 300-304.
23. Sun, X.Z., et al., *Cell-cycle synchronization of fibroblasts derived from transgenic cloned cattle ear skin: effects of serum starvation, roscovitine and contact inhibition*. Zygote, 2008. **16**(2): 111-116.
24. Zamir, E. and B. Geiger, *Molecular complexity and dynamics of cell-matrix adhesions*. Journal of Cell Science, 2001. **114**(20): 3583-3590.
25. Bates, E.F.M., et al., *Identification and analysis of a novel member of the ubiquitin family expressed in dendritic cells and mature B cells*. European Journal of Immunology, 1997. **27**(10): 2471-2477.

26. Rat Genes, RGD ID 620717, Rat Genome Database Web Site. February 2009, *Medical College of Wisconsin, Milwaukee, Wisconsin*: <http://rgd.mcw.edu/>.
27. Kato, G. and S. Maeda, *High-level expression of human c-Src can cause a spherical morphology without loss of anchorage-dependent growth of NIH 3T3 cells*. Federation of European Biochemical Societies Letters, 1997. **411**(2-3): 317-321.
28. Thomas, P.D., et al., *PANTHER: A library of protein families and subfamilies indexed by function*. Genome Research, 2003. **13**(9): 2129-2141.
29. McLeod, S.J., et al., *The Rap GTPases regulate integrin-mediated adhesion, cell spreading, actin polymerization, and Pyk2 tyrosine phosphorylation in B lymphocytes*. Journal of Biological Chemistry, 2004. **279**(13): 12009-12019.